







Preoperative planning of supramaleolar deformities correction through 3D printing

Tiago Baumfeld¹ , Ricardo Fernandes Rezende² , Luiza Helena Oliveira e Araújo¹ , Marco Antonio Percopo de Andrade¹ , Daniel Baumfeld¹ , Rudolf Huebner¹ 

ABSTRACT

3D printed models have been explored deeply in the medical field, standing out as an important aid tool for surgical planning. The authors present a case report of a patient with post-traumatic arthrosis of the right ankle, who underwent supramaleolar osteotomy, using a medial closure wedge. This surgery was performed after operative planning by 3D printing, which can demonstrate the reproducibility of this method.

Keywords: Ankle; Three-dimensional printing; Surgical procedures; Osteotomy.

1. Universidade Federal de Minas Gerais, (MG), Brasil
2. Hospital Felício Rocho - Belo Horizonte, (MG), Brasil



INTRODUCTION

Three-dimensional (3D) printing was first described by Charles W. Hull in 1986, and has been used extensively for the past 30 years¹. Due to its precise reconstruction of complex anatomical structures, the use of 3D printing in medicine is increasing, being used for the learning of basic anatomy to advanced surgical practice². Educational models including bones were built using 3D printing technology³. Most of the reported 3D printed models are highly accurate and realistic. However, they have limitations, mainly related to the choice of hardware, software, and materials to be used. In addition, these models may not translate the damage to the articular cartilage, since they come from a CT scan^{2,4,5}.

Currently, 3D printed models have been explored deeply in the medical field with the advantages of shortening the learning curve for surgeons and assisting them in better planning of complex surgical procedures^{2,3,5}. As an example, we cite the work carried out by Feng Shuang et al, using personalized 3D printed osteosynthesis plates demonstrating the safety and efficacy of this method for the treatment of intercondylar fractures of the humerus, significantly reducing the operative time⁶.

Supramaleolar osteotomy is a surgical procedure commonly used to correct congenital or acquired deformities of the distal region of the tibia^{7,8}. Currently, supramaleolar osteotomy has been widely used to treat asymmetric ankle arthrosis, as a preservative surgical method, aiming at realignment and redistribution of loads on the ankle and making it a good option for arthrodesis and arthroplasty, in some cases^{9,10,11,12}.

The purpose of this case report was to demonstrate the use of a three-dimensional (3D) impression model in the surgical planning of a supramaleolar osteotomy of the ankle in a patient with tibiotarsal osteoarthrosis.

CASE REPORT

The patient duly signed the free and informed consent form, agreeing and authorizing the disclosure of the data obtained from medical records, as well as the images and photos shown in this case report. In addition, bioethical approval was obtained from the Research Ethics Committee (CAAE: 18913219.0.0000.5125).

We present the case of a 22-year-old male patient, working as a vigilant. He had a history of trauma, with an ankle fracture treated conservatively in another service two years before the first assessment. At the time of the consultation, he reported severe pain in his right ankle, difficulty walking and practicing physical activities, feeling of stiffness and crackling.

On physical examination, he had intact skin, without scarring, absence of signs of infection, preserved distal perfusion, absence of motor and sensory deficit, valgus deformity in the distal region of the leg, 50° range of motion and pain on palpation of the medial region of the ankle.

Weight-bearing radiographs of the right ankle (AP and lateral) and computed tomography (CT) showed post-traumatic arthrosis of the right ankle, classified as Takakura stage 3A and a Lateral Distal Tibia Angle (LDTA) of 100°^{9,10,13} (Figure 1).



Figure 1 A) weight-bearing AP radiograph of the right ankle. B) CT scan of the right ankle (coronal view).

The patient reported that he had undergone conservative treatment in the last year in an intense way, having done more than 100 sessions of physiotherapy, water aerobics, hyaluronic acid infiltration and use of various oral medications, including glucosamine, diacerein and collagen. The patient reported that he was unhappy due to ankle disability and wished to undergo a surgical procedure to improve his condition.

Due to supramaleolar valgus deformity and Takakura 3A arthrosis classification, a joint preservative surgery, a supramaleolar osteotomy (SMOT) with a

medial closure wedge¹⁴ was chosen. This technique was chosen due to the initial correction planning 10°, which does not require osteotomy of the fibula for its complementation. This decision followed the most recent protocols for this surgery, and was also supported by the benefits of a medial closure osteotomy in relation to the lateral opening wedge, such as its greater technical ease, its better consolidation rates, the absence of need for using graft and possibility of accurate planning with a 3D model^{14,15,16}.

SMOT is a technique whose results depend on the accuracy of correction of the deformity¹⁶ and for that it was chosen to perform preoperative surgical planning in a 3D model. To make the model, the CT whose LDTA angle in the coronal plane was 100°, was worked using the software InVesalius, Meshmixer and Slic3r. The pieces were arranged to be printed, defining their printing parameters (internal geometry density of 10%, internal grid fill shape, layer height 0.25mm, wall thickness 3mm). Ahead, the pieces were sliced, generating the G-code file (Figure 2).

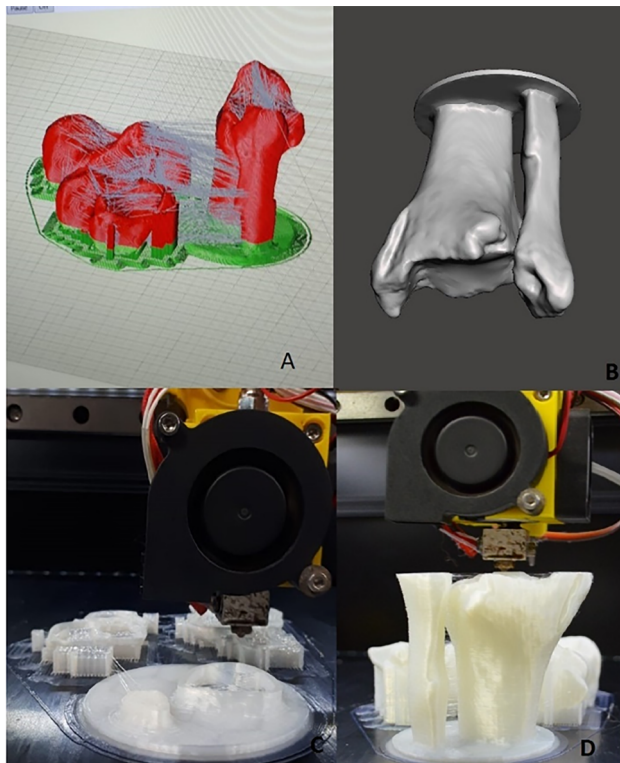


Figure 2 (A / B) Tomography modeling. (C / D) 3D part printing.

The printers used: Factor 3D P350 and Sethi 3D AIP A3. The material used for printing was the PLA filament (lactic polyacid); cross-sectional diameter 1.75mm; extrusion temperature 190°C to 210°C. The printing time was 8 hours. In the laboratory, with the 3D part, the LDTA angle was again measured, whose value was confirmed at 100°.

The model was then taken to the laboratory where preoperative planning was carried out. A 1 cm long medial tibial wedge osteotomy was performed, 2 cm proximal to the apex of the medial malleolus. These parameters were chosen to achieve the CORA of the deformity and to correct the LDTA angle to 90°, as recommended in literature^{14,15,16}. It is assumed that each millimeter of the wedge corrects a degree of deformity¹⁵. The osteotomy was then fixed medially with a T-plate, with 4 holes, with a pre-molded 3.5 mm profile, and 8 screws with bicortical fixation, being 4 cortical screws, size 45 mm, 1 cortical screw size 30 mm and 3 blocked screws size 30 mm. Previously, a tubular third plate, 5-hole, 3.5 mm profile plate was positioned with 4 screws, 2 of which were blocked with 28 mm, 1 with 28 mm and 1 with 40 mm. (Figure 3). All screw sizes have been documented and the plates have been molded. The screws used in this laboratory planning were reserved for sterilization to be used in vivo. The planning had a total duration of 30 minutes.

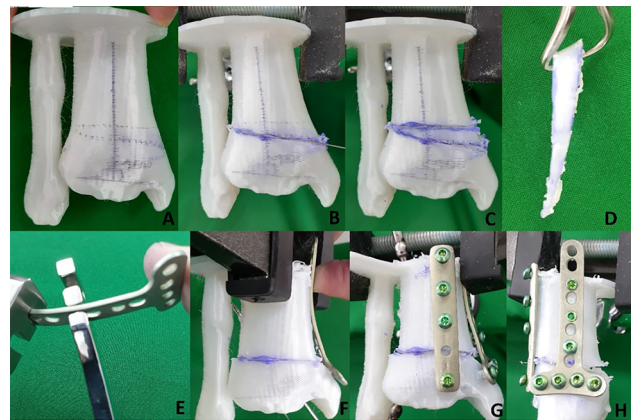


Figure 3 (A) Drawing of the LDTA angle and the wedge on the 3D part. (B / C) Wedge on the 3D part. (D) Wedge. (E) Pre-molding the T-plate. (F) 3D part without the wedge. (G) 3D part with osteosynthesis materials. (H) 3D piece with osteosynthesis materials.

At the end of the planning, an LDTA angle of 90° ¹³ was obtained. The objective was a hypercorrection following the recommendations of the literature^{14,15,16}.

Five days after planning in the laboratory, the patient underwent surgery. Under spinal anesthesia, the patient was placed in the supine position. After insufflation of a tourniquet, a medial incision was made over the tibia with extension to the medial malleolus to perform the medial closure wedge SMOT, 1 cm long, 2 cm proximal to the apex of the medial malleolus using the same instruments, plates and screws used in the 3D part. The size of the removed wedge was the same as that obtained in the planning (10 mm). (Figure 4). After radioscopy control, conventional closure and placement of a plastered bandage was performed. The surgery had a total duration of 45 minutes. The LDTA angle on AP radiography obtained on fluoroscopy, 30 and 90 days after surgery, was 90° (Figure 5).

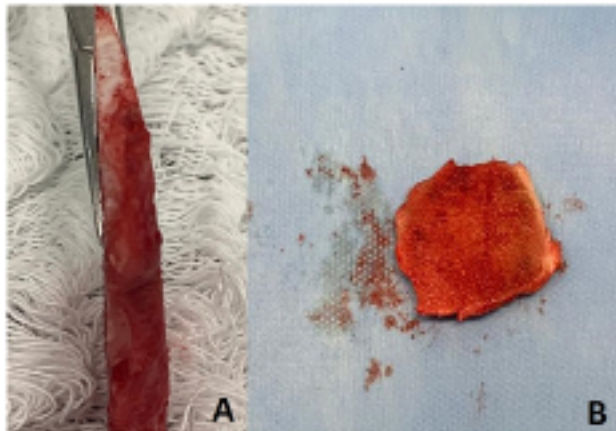


Figure 4 Wedge removed in the surgery.

Due to the stability obtained with the medial plate, it was decided during the intraoperative period not to place the anterior plate. We used the same pre-molded medial plate and the same screws, demonstrating the reproducibility of the surgical planning by 3D printing.

The postoperative period was conducted on an outpatient basis with the splint maintained for 21 days, the stitches were removed at the same time, and transitioned to a boot. Proprioceptive support was started at 6 weeks progressing to full support at 10 weeks. Physiotherapy was started in the third week and maintained until the end of the fourth postoperative month. Impact activities were released after total consolidation of the osteotomy and the patient's clinical comfort, which occurred at 6 months of follow-up.

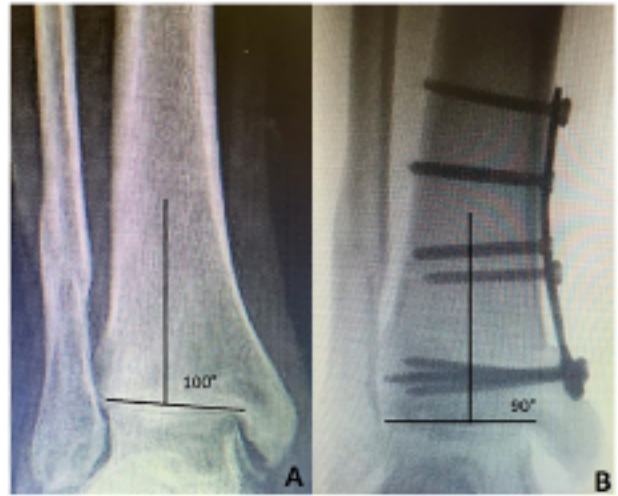


Figure 5 (A) Preoperative AP radiograph of the ankle. (B) Postoperative AP radiograph of the ankle showing correction of the TAS angle.

DISCUSSION

In the present case report, an LDTA angle of 100° was obtained in the preoperative CT and the 3D part before planning. After planning, a 90° LDTA value was obtained, which corresponds to the LDTA on the postoperative radiography. In addition, there was no need to change the number and size of any of the screws and the pre-molded medial plate. When performing a distal osteotomy, the surgeon's objective should be to restore the LDTA (VR: $86-92^\circ$) back to the values compared with the contralateral limb and / or slight overcorrection with $2-4^\circ$ of varus¹⁷. This shows that 3D models are highly accurate.

L. Maini et al. in a randomized, prospective case-control study evaluated the precision of molded and specific plates for patients with acetabular fractures. Twenty-one patients were included (10 in the "case" group and 11 in the "control" group). In the "case" group, a real 3D model specific to the patient plate for the fractured acetabulum was made using rapid prototyping technology and pre-molding of plates in the preoperative period. The control group was treated using plates molded intraoperatively. The authors observed a reduction in blood loss of 100 ml, a reduction in surgical time of 12 min and better functional results in the "case" group¹⁸. The authors concluded that plates made for each patient, using 3D printed models, are superior during the intraoperative period because they are more accurate.

Bagaria V et al. in his work on the treatment of complex fracture of the acetabulum, calcaneus and medial condyle of the femur (Hoffa fracture),

using preoperative planning similar to the previous one, reported an improvement in the understanding of the fracture configuration. In addition, the authors believe that there was an indirect reduction in surgical time, decreased need for anesthetic and decreased intraoperative blood loss¹⁹. Similar results were also found by other authors^{20,21}. In our study, we verified the precision obtained with three-dimensional planning, and we also believe that there was a decrease in surgical time and blood loss, but it was not possible to quantify these data.

There is an increase in the use of 3D printed models in Brazil, not only in medicine, but also in veterinary medicine, dentistry and other areas^{22, 23, 24}. Advances in the medical field already allow obtaining blood vessel networks and bioprinted liver organelles, used for training surgeons and drug toxicity studies, respectively. There have also been advances in the manufacture of personalized orthoses for bodily injuries^{25,26,27}.

We chose not to use the anterior plate in the intraoperative period because we do not believe it would add stability to the system. The size of the screws used was determined objectively by measuring between the two cortices.

We emphasize the need for a careful evaluation of the implants before the surgical procedure, since there is a risk of damaging them during planning. One option would be to use the model plate only as a template, but the increase in costs may make the procedure unfeasible.

We highlight here some of the limitations presented by this study. We emphasize the need for studies, such as larger and prospective cohorts, so that aspects such as surgical time, the accuracy of measurements, blood loss and implant stability can be evaluated. Another aspect of being considered is choosing of the material to be used while making the 3D piece. Polylactic acid (PLA), the material used in this case, despite being biodegradable and having a low cost, has low resistance to tension forces, being a fragile and inelastic material, as well as Polyethylene Terephthalate (PET)^{28,29}. This property limits its use in situations that require plastic deformation and high levels of stress, such as fixing fractures with screws and plates³⁰.

CONCLUSION

3D parts can prove to be highly accurate and contribute to the planning of orthopedic surgeries, adding direct benefits, such as accuracy in correcting deformities, shaping the plate and choosing the size of the screws.

REFERENCES

- Hull, C. W. Apparatus for production of three-dimensional objects by stereolithography (1996).
- Collin E Pehde , John Bennett , Brad Lee Peck, Logan Gull. Development of a 3-D Printing Laboratory for Foot and Ankle Applications. *Clin Podiatr Med Surg*. 2020 Apr;37(2):195-213. doi: 10.1016/j.cpm.2019.12.011.
- Akhil Sharma, Kyle S Kirkland, Robert M Holloway, Selene G Parekh. Incorporating 3D Printing Into Your Practice: Lessons Learned. *Foot Ankle Spec*. 2020 Dec 20;1938640020980912. doi: 10.1177/1938640020980912.
- Wang L, Ye X, Hao Q, Chen Y, Chen X, Wang H, et al. Comparison of two three-dimensional printed models of complex intracranial aneurysms for surgical simulation. *World Neurosurg*. 2017;103:671-679.
- Waran V, Narayanan V, Karupiah R, Owen SL, Aziz T. Utility of multimaterial 3D printers in creating models with pathological entities to enhance the training experience of neurosurgeons. *J Neurosurg*. 2014;120:489-492.
- Feng Shuang, MD, Wei Hu, MD, Yinchu Shao, MD, Hao Li, MD, and Hongxing Zou, MD. Treatment of Intercondylar Humeral Fractures With 3D-Printed Osteosynthesis Plates. *Medicine* _ Volume 95, Number 3, January 2016.
- Abraham E, Lubicky JP, Songer MN, et al. Supramalleolar osteotomy for ankle valgus in myelomeningocele. *J Pediatr Orthop* 1996;16(6):774-81.
- Nicol RO, Menelaus MB. Correction of combined tibial torsion and valgus deformity of the foot. *J Bone Joint Surg Br* 1983;65(5):641-5.
- Takakura Y, Tanaka Y, Kumai T, Tamai S. Low tibial osteotomy for osteoarthritis of the ankle. Results of a new operation in 18 patients. *J Bone Joint Surg Br* 1995;77(1):50 -4. 486 R.A. Benthien, M.S. Myerson / *Foot Ankle Clin N Am* 9 (2004) 475-487
- Takakura Y, et al. Results of opening-wedge osteotomy for the treatment of a post-traumatic varus deformity of the ankle. *J Bone Joint Surg Am* 1998;80(2):213 -8.
- Stamatis ED, Cooper PS, Myerson MS. Supramalleolar osteotomy for the treatment of distal tibial angular

- deformities and arthritis of the ankle joint. *Foot Ankle Int* 2003;24(10):754–64
12. Tarr RR, Resnick CT, Wagner KS, et al. Changes in tibiotalar joint contact areas following experimentally induced tibial angular deformities. *Clin Orthop* 1985; 199:72–80.
 13. Mangone PG. Distal tibial osteotomies for the treatment of foot and ankle disorders. *Foot Ankle Clin*. 2001;6(3):583-97.
 14. Beat Hintermann, MD, Markus Knupp, MD, Alexej Barg, MD. Supramalleolar Osteotomies for the Treatment of Ankle Arthritis. *Journal of the American Academy of Orthopaedic Surgeons*. July 2016, Vol 24, No 7.
 15. Adam S. Becker, MD^{a,b}, Mark S. Myerson, MD^{a,*}. The Indications and Technique of Supramalleolar Osteotomy. *Foot Ankle Clin N Am* 14 (2009) 549–561 doi:10.1016/j.fcl.2009.06.002.
 16. Ross A. Benthien, MD, Mark S. Myerson, MD^{*}. Supramalleolar osteotomy for ankle deformity and arthritis R.A. Benthien, M.S. Myerson / *Foot Ankle Clin N Am* 9 (2004) 475–487.
 17. Hintermann B, Barg A, Knupp M: Corrective supramalleolar osteotomy for malunited pronation-external rotation fractures of the ankle. *J Bone Joint Surg Br* 2011;93(10):1367-1372.
 18. L. Maini¹ · A. Sharma^{1,3} · S. Jha² · A. Sharma¹ · A. Tiwari¹. Three-dimensional printing and patient-specific pre-contoured plate: future of acetabulum fracture fixation?. *Eur J Trauma Emerg Surg*. DOI 10.1007/s00068-016-0738-6.
 19. Bagaria V, Deshpande S, Rasalkar DD, Kuthe A, Paunipagar BK. Use of rapid prototyping and three-dimensional reconstruction modeling in the management of complex fractures. *Eur J Radiol*. 2011;80:814–20.
 20. Qipeng Wu, Tao Yu, Bo Lei, Wenjie Huang, Ruokun Huang. A New Individualized Three-Dimensional Printed Template for Lateral Ankle Ligament Reconstruction. *Med Sci Monit*. 2020 Mar 5;26:e922925. doi: 10.12659/MSM.922925.
 21. Anil Murat Ozturk, Onur Suer, Istemihan Coban, Mehmet Asim Ozer, Figen Govsa. Three-Dimensional Printed Anatomical Models Help in Correcting Foot Alignment in Hallux Valgus Deformities. *Indian J Orthop*. 2020 Apr 23;54(Suppl 1):199-209. doi: 10.1007/s43465-020-00110-w. eCollection 2020 Sep.
 22. Reis, D. de A. L. dos, Gouveia, B. L. R., Alcântara, B. M. de, Saragiotto, B. P., Baumel, Érica E. D., Ferreira, J. S., Rosa Júnior, J. C., Oliveira, F. D. de, Santos, P. R. da S., & Assis Neto, A. C. de. (2017). Biomodelos Ósseos Produzidos por Intermédio da Impressão 3D: Uma Alternativa Metodológica no Ensino da Anatomia Veterinária. *Revista De Graduação USP*, 2(3), 47-53. <https://doi.org/10.11606/issn.2525-376X.v2i3p47-53>.
 23. Ana Luísa Bettega, AcCBC-PR, Luis Fernando Spagnuolo Brunello, AcCBC-PR, Guilherme Augusto Nazar, Giovanni Yuji Enomoto De-Luca, Lucas Mansano Sarquis, AcCBC-PR, Henrique de Aguiar Wiederkehr, AcCBC-PR, José Aguiomar Foggiatto, Silvania Klug Pimentel, TCBC-PR. Simulador de dreno de tórax: desenvolvimento de modelo de baixo custo para capacitação de médicos e estudantes de medicina. *Rev. Col. Bras. Cir.* vol.46 no.1 Rio de Janeiro 2019. <https://doi.org/10.1590/0100-6991e-20192011>.
 24. J.V.P. Bertti, E.E. Silveira, A.C. Assis Neto. Reconstrução e impressão 3D do neurocrânio de cão com o uso de tomografia computadorizada como ferramenta para auxiliar no ensino da anatomia veterinária. *Arq. Bras. Med. Vet. Zootec.* vol.72 no.5 Belo Horizonte Sept./Oct. 2020 Epub Nov 09, 2020. <https://doi.org/10.1590/1678-4162-11209>.
 25. Glen S. Van Arsdell, MD^{a,b}, Nabil Hussein, MBChB^{c,d}, and Shi-Joon Yoo, MD^{c,e}. Three-dimensional printing in congenital cardiac surgery—Now and the future. *The Journal of Thoracic and Cardiovascular Surgery* 2020 ; 1-5. <https://doi.org/10.1016/j.jtcvs.2019.12.131>.
 26. Nguyen DG, Funk J, Robbins JB, Crogan-Grundy C, Presnell SC, Singer T, et al. Bioprinted 3D primary liver tissues allow assessment of organ-level response to clinical drug induced toxicity in vitro. *PLoS One*. 2016;11: 1-17. 3.
 27. Liacouras P1, Garnes J, Roman N, Petrich A, Grant GT. Designing and manufacturing an auricular prosthesis using computed tomography, 3-dimensional photographic imaging, and additive manufacturing: a clinical report. *J Prosthet Dent*. 2011;105:78-82.
 28. R. AURAS, B. HARTE, S. SELKE, An overview of polylactides as packaging materials. *Macromol. Biosci.* v. 4, p. 835–864, 2004.
 29. RASAL, R.M.; HIRT, D.E. Toughness decrease of PLA-PHBHHx blend films upon surface-confined photopolymerization. *J. Biomed. Mater. Res. Part v. 88 A*, p. 1079–1086, 2008.
 30. RASAL, R.M.; JANORKAR, A.V.; HIRT, D.E. Poly(lactic acid) modifications, *Prog. Polym. Sci.* v. 35, p. 338–356, 2010.

Interest conflicts:

None of the authors have conflicts of interest.

Finance: None.

Corresponding Author:

Ricardo Fernandes Rezende

ricardomed1992@gmail.com

Editor:

Prof. Dr. Marcelo Riberto

Received in: jul 52, 2020

Approved in: feb 12, 2021
